serval
serveur académique lausannois

Unil
UNIL | Université de Lausanne
Faculty of Biology and Medicine

CHUV

Kir5.1 regulates Nedd4-2-mediated ubiquitination of Kir4.1 in distal nephron

Ming-Xiao Wang[1,2], Xiao-Tong Su[2], Peng Wu[2], Zhong-Xiuzi Gao[2], Wen-Hui Wang[2], Olivier Staub*, Dao-Hong Lin[2]

1: Department of Physiology, Zunyi Medical College, Zunyi, China, 2: Department of Pharmacology, New York Medical College, Valhalla, NY, USA and *Department of Pharmacology and Toxicology, University of Lausanne, 1005 Lausanne, Switzerland.

Corresponding Address:
Dr. Dao-Hong Lin
Department of Pharmacology
New York Medical College
15 Dana Road
Valhalla, NY, 10595
Email: daohong_lin@nymc.edu
Tel: 914-594-3870
Fax: 914-347-4956

Running title

Nedd4-2 regulates Kir4.1/Kir5.1

Key words

Kcnj10, Kcnj16, Nedd4-1, NCC, EAST/SeSAME syndrome

Abstract

Kir4.1/5.1 heterotetramer participates in generating the negative cell membrane potential in distal convoluted tubule (DCT) and plays a critical role in determining the activity of Na-Cl co-transporter (NCC). Kir5.1 contains a phosphothreonine-motif at its c-terminus (AA249-252). Co-immunoprecipitation showed that Nedd4-2 was associated with Kir5.1 in HEK293 cells cotransfected with Kir5.1 or Kir4.1/Kir5.1. GST-pull-down further confirmed the association between Nedd4-2 and Kir5.1. Ubiquitination assay showed that Nedd4-2 increased the ubiquitination of Kir4.1/Kir5.1 heterotetramer in the cells co-transfected with Kir4.1/Kir5.1 but it has no effect on Kir4.1 or Kir5.1 alone. Patch-clamp and western blot also demonstrated that co-expression of Nedd4-2 but not Nedd4-1 decreased K currents and Kir4.1 expression in the cells cotransfected with Kir4.1 and Kir5.1. In contrast, Nedd4-2 fails to inhibit Kir4.1 in the absence of Kir5.1 or in the cells transfected with the inactivated form of Nedd4-2 (Nedd4-2C821A). Moreover, the mutation of TPVT motif in the C-terminus of Kir5.1 largely abolished the association of Nedd4-2 with Kir5.1 and abolished the inhibitory effect of Nedd4-2 on K currents in HEK293 cells transfected with Kir4.1 and Kir5.1 mutant (Kir5.1T249A). Finally, the basolateral K conductance in the DCT and Kir4.1 expression is significantly increased in the kidney-specific Nedd4-2 knockout or in Kir5.1 knockout mice in comparison to their corresponding WT littermates. We conclude that Nedd4-2 binds to Kir5.1 at phosphothreonine-motif of the c-terminus and the association of Nedd4-2 with Kir5.1 facilitates the ubiquitination of Kir4.1 thereby regulating its plasma expression in the DCT.

Introduction

Kir4.1 (encoded by *Kcnj10*) is an inwardly-rectifying K channel which interacts with Kir5.1 (encoded by *Kcnj16*) to form a 40 pS K channel in the basolateral membrane of the distal convoluted tubule (DCT)(14; 18; 28). Because this 40 pS K channel is the only type of K channel in the basolateral membrane of the DCT(28; 35), it plays a key role in generating negative membrane potential and handling K recycling. Previous studies have demonstrated that the deletion of Kir4.1 completely eliminated the basolateral K conductance and depolarized the membrane of the DCT (35). Kir4.1/Kir5.1 channel activity in the DCT plays a key role in determining the expression of Na-Cl cotransporter (NCC) and in mediating the effect of dietary K intake on NCC through a Cl-sensitive with-no-lysine kinase (WNK) pathway (2; 4; 19; 35). Since NCC plays a role not only in reabsorption of 5% of the filtered Na load but also in regulating renal K excretion (8; 16), the modulation of Kir4.1/5.1 channel activity should have a profound effect on renal Na and K handing(5).

While Kir4.1 is a K-conductive component for the Kir4.1/5.1 heterotetramer (18), the role of Kir5.1 in forming the heterotetramer is not completely understood. It has been demonstrated that Kir5.1 may regulate the pH sensitivity of the basolateral K channels in the DCT (17; 18). The analysis of Kir5.1 amino acid sequence reveals that Kir5.1 contains a phosphothreonine-motif (TPVT) at its c-terminus (AA249-252) which has been shown to bind to E3 ubiquitin ligase Nedd-4 (15). The main isoform of Nedd4-2 E3 ligase in the aldosterone-sensitive distal nephron is Nedd4-2(21). Nedd4-2 is a HECT-domain containing E3 ligase and plays a profound role in regulating ubiquitination of a variety of ion transporters, such as NCC and ENaC (21; 22; 36). Nedd4-2 contains a C2 domain and four WW domains which confer protein interaction with the substrate protein. Nedd4-2 selects and recruits the substrate protein not only by binding to canonical PY motif of the substrate protein through its specific WW domain but also to phospho-threonine/serine motif (1; 15). This study is aimed at exploring whether Kir5.1 is a binding component for Nedd4-2 thereby regulating Kir4.1 ubiquitination in the DCT.

Methods

Animals   We used *Kcnj16*$^{+/+}$ (Kir5.1 WT), *Kcnj16*$^{-/-}$ (Kir5.1 knockout) mice with C57bl/6 background, inducible kidney-specific Nedd4-2 deletion (Ks-Nedd4-2 KO) and *Nedd4l*$^{flox/flox}$ (WT control for Ks-Nedd4-2 KO) mice with C57bl/6 background for the experiments. We have purchased male and female *Kcnj16*$^{+/-}$ mice from Mary Lyon Center (Oxfordshire, UK) for breeding in the animal facility of New York Medical College. After genotyping, we used both 8 week-old male or female *Kcnj16*$^{-/-}$ and *Kcnj16*$^{+/+}$ mice for experiments. To generate Ks-Nedd4-2 KO mice, mice expressing Pax8-rtTA and tet-on LC-1 transgene were crossed with *Nedd4l*$^{flox/flox}$ mice which were originally generated in O. Staub's laboratory (22). *Nedd4l* deletion was carried out in 8-week-old male and/or female mice homozygous for floxed *Nedd4l* gene and heterozygous for Pax8-rtTA/LC-1 transgene by providing doxycycline (5mg/ml, 5% sucrose) in the drinking water for 2 weeks. This was followed by at least 2 additional weeks without doxycycline treatment before performing experiments. Littermate mice of the same age and genetic background and drinking 5% sucrose were used as controls (*Nedd4l*$^{flox/flox}$). Genotyping confirms the positive strain Nedd4-2cre-flox. The primers for genotyping were listed in Table 1. All the procedures were reviewed and approved by the Institutional Animal Care and Use Committee (IACUC).

Preparation of the DCT   Mice were sacrificed by cervical dislocation and the abdomen was opened to expose the left kidney. We perfused the left kidney with 2 ml L-15 medium (Life Technology) containing Type 2 collagenase (250 U/ml) and then removed the collagenase-perfused kidney. The renal cortex was separated and further cut into small pieces for additional incubation in collagenase-containing L-15 media for 30-50 min at 37°C. The tissue was then washed three times with fresh L-15 medium and transferred to an ice-cold chamber for dissection. The isolated DCT tubules were placed on a small cover glass coated with poly-lysine and the cover glass was placed on a chamber mounted on an inverted microscope.

Cell culture and Gene Transfection   HEK293 cells (ATCC, Manassas, VA) were used for transient expression of Kir4.1, Kir5.1 and Nedd4-1 or Nedd4-2. The cells were grown in Dulbecco's modified Eagle

4

medium (DMEM; Invitrogen) supplemented with 10% FBS (Invitrogen) in 5% CO_2 and 95% air at 37°C. Cells were grown to 50–70% confluence for transfection as described previously (34). Briefly, a cDNA cocktail (total 2 µg) was prepared with 200 µl serum free DMEM and 6 µl Turbofect transfection reagent (Thermo Fisher Scientific) for the cells in a 35 mm dish. Cells transfected with the empty vector were used as IgG control for immunoprecipitation (IP) and their background currents were subtracted from that of the experimental groups for patch-clamp study. After 15 min incubation at room temperature, the mixture of the transfection cocktail was applied to the cells followed by additional 24 h incubation before use.

Co-immunoprecipitation (CO-IP) and Ubiquitination assay   IP was performed as previously described(13). Briefly, 200 µg total protein was mixed with 2 µg of the IP antibody in 200 µl of 1% PBST. The mixture was incubated with overnight shaking at 4°C and followed by adding 50 µl of protein A agarose (Santa Cruz Biotechnology, Dallas, TX) and mixing gently with shaking for an additional hour. The agarose was pelleted and ready for SDS-PAGE gel examination.

For the ubiquitination assay, 2% SDS was added into 200 µg total protein lysate. The sample was incubated for 5 min at 95°C and diluted 10 times with lysate buffer before conducting immunoprecipitation (IP). The IP antibody was added into the lysate as in the protocol described above.

Site-directed mutagenesis   The over-lapping PCR-based mutagenesis method was used to generate Kir5.1 mutants (UniProtKB-Q9NPI9-Human). Two pairs of complementary primers harboring the mutant site Kir5.1T249A or –T249D were phosphorylated by T4 polynucleotide kinase at 37 °C. We used 20 ng of pcDNA3-Flag-Kir5.1 as template. A 50 µl PCR reaction was set up routinely, including with LA-Taq and DNA ligase. After PCR product was incubated with DpnI for 1 h, 1 µl PCR product was used for transformation. Mutant plasmid DNA was verified by sequencing.

Whole cell recording with patch clamp   Borosilicate glass (1.7-mm OD) (Harvard Apparatus, Holliston, MA USA) was used to make the patch-clamp pipettes that were pulled with a Narishige electrode puller (Narishige, Long Island, NY, USA). The pipette had a resistance of 2 to 4 MΩ when filled with 140 mM

KCl. The tip of the pipette was filled with pipette solution containing 140 mM KCl, 2 mM $MgCl_2$, 1 mM EGTA, and 5 mM HEPES (titrated with KOH, pH=7.4). The pipette was then back-filled with pipette solution containing amphotericin B (20 μg/0.1 mL). For measurement of Ba^{2+}-sensitive K currents, the cells were incubated with a bath solution containing 140 mM KCl, 2 mM $MgCl_2$, 1.5 mM $CaCl_2$, and 5 mM HEPES (titrated with KOH, pH=7.4). After forming a high-resistance seal (>2 GΩ), the membrane capacitance was monitored until the whole-cell patch configuration was formed. The cell membrane capacitance was measured and compensated. This compensated value indicated the membrane capacitance of each cell and it was used for normalizing K currents for each measurement. K currents were measured by an Axon 200A patch-clamp amplifier (Molecular Devices, Sunnyvale, CA, USA). The currents were low-pass filtered at 1 KHz and digitized by an Axon interface (Digidata 1320, Molecular Devices). Data were stored in a Dell PC and analyzed using the pClamp software version 9 at sampling rate of 4K Hz (Molecular Devices). K current measured in HEK cells was presented as picoamperes (pA)/30 picofarads (pF) while it was pA per DCT cell.

GST pull down   Four WW domains of Nedd4-2 and full length of Kir5.1 were individually inserted into pGEX4T-1 vector. C-terminal of Kir5.1 was inserted into pET19b vector. The primers used for the procedures were listed in Table 2. The constructs were confirmed by sequencing. For the induction of expression, 10 ml BL21 E. coli containing the transformed plasmid pGEX4T-1-WW domain proteins or pET19b-Kir5.1-C-terminus were induced by IPTG (0.2 mM) for 4-5 hr. Cell pellets were lysed with BugBuster protein extraction buffer (EMD Millipore, Billerica, MA). Supernatant was taken after centrifuging. Total protein concentration was quantified. 200 μg total GST protein was mixed with 50 μl of washed Glutathione beads (Thermo Fisher Scientific). After shaking at 4 °C for 2 h, we added 200 μg total protein containing flag-tagged-Nedd4-2 obtained from TNT T7 Quick Coupled Translation System (Promega, Madison, WI) into GST-proteins for overnight incubation. The mixture was washed three times with 1% PBST and the beads were loaded to PAGE-SDS gel.

Immunofluorescent staining   Mice were anesthetized and perfused with 30 mL PBS containing heparin (40 unit/mL) followed by 100 mL of 4% paraformaldehyde. After perfusion, the kidneys were embedded and cut into 7 μm slices with Leica1900 cryostat (Leica). The slides were washed with 1× PBS for 15 min, and permeabilized with 1× PBS buffer containing 0.3% Triton X100, 1% BSA and 0.1% lysine (pH = 7.4) for 15 min. Kidney slices were blocked and incubated with primary antibodies (Kir4.1) for 24 h at 4 °C. Immunostaining was examined with Olympus inverted microscope DP73.

Antibodies and reagents   We purchased primary antibodies for HA and Ub4D1 from Covance (Dedham, MA), for Nedd4-2 from Cell Signaling Technologies (Beverly, MA, USA), for monoclonal Flag from Sigma, for Kir4.1 and Kir5.1 from Alomone Labs (APC-123) (Jerusalem, Israel). We also obtained Kir5.1 antibody (repeat and validate the results from APC-123) from Santa Cruz Biotechnology (SC-30151) (Dallas, TX) and α-Tubulin and GFP from Rockland (Limerick, PA). We purchased second antibodies including IRDye® 800CW Goat anti-Mouse IgG, IRDye® 680RD Goat anti-Rabbit IgG from LI-COR. All antibodies were validated by using corresponding genetic modified animals (for Kir4.1 and Kir5.1) or previous experimental information. All chemicals and proteinase/phosphatase inhibitors were purchased from Sigma Aldrich (St. Louis, MO) unless otherwise specified.

Statistics analysis   Student's *t*-test (unpaired groups) was used to determine the significance of differences between two groups or one-way analyses of variance (ANOVA) was used to determine the statistical significance among multiple groups. Holm-Sidak was used as post hoc test. *P*<0.05 was defined as statistical significance.

Results

Kir5.1 interacts with Nedd4-2.   We first examined the interaction between Kir5.1 and Nedd4-2 with CO-IP in HEK293 cells transfected with HA-GFP-tagged Kir5.1 and Flag-tagged Nedd4-1 or Nedd4-2. We used Flag antibody (precipitating either Nedd4-2 or Nedd4-1) for IP and HA antibody (detecting Kir5.1) for blotting. Fig.1A shows that Nedd4-2/Kir5.1 interaction (top panel) was stronger than Nedd4-1/Kir5.1

interaction , suggesting that Kir5.1 is mainly associated with Nedd4-2. Fig.1A also shows equal expression of Flag-tagged Nedd4-2 or Nedd4-1(middle panel) and HA-GFP tagged Kir5.1 (lower panel). We next conducted CO-IP with myc antibody in the cells transfected with myc-his-tagged Kir5.1 and Flag-Nedd4-2 or –Nedd4-1. Fig.1B is a western blot showing that myc-Kir5.1 was predominantly associated with Nedd4-2. After demonstrating that Kir5.1 was able to bind to Nedd4-2, we next examined the binding site of Kir5.1 with Nedd4-2. Although Kir5.1 has no typical PY motif, it has a phosphothreonine motif in the c-terminus (TPVT from amino acid sequence 249-252) which has been shown to be a binding site for Nedd4 in M-phase inducer phosphatase 3 (15). To test the possibility, we conducted CO-IP with flag antibody in the cells transfected with Kir5.1^{T249A} in which threonine was mutated to alanine. As shown in Fig. 1C (top panel), the mutation (Kir5.1^{T249A}) decreased the binding of Kir5.1 with Nedd4-2. From 4 separate experiments it is calculated that T249A mutation significantly decreased the association between Kir5.1/Nedd4-2 from WT control 1.10±0.15 (normalized band density) to 0.50±0.24 (Fig.1E). In contrast, mutating Thr^{249} into Aspartate (D) slightly enhanced association (band density=1.36±0.10) although this was not significantly different from (Kir5.1) control (1.10±0.15) (Fig.1E). In contrast, the mutation of Thr^{252} to either Ala (1.07±0.11) or Asp (1.18±0.09) did not significantly affect the interaction between Kir5.1 and Nedd4-2 (Fig.1D). Thus, the results suggest that TPVT motif of Kir5.1 is a binding site for Nedd4-2.

To further test for the interaction between Nedd4-2 and Kir5.1 in vitro, we conducted GST pull-down experiments using purified GST fusion proteins from prokaryotic cells. From the inspection of Fig.2A, it is apparent that full-length GST-tagged Kir5.1 protein binds to Flag-tagged Nedd4-2 while GST protein failed to pull down Nedd4-2. Moreover, GST-pull-down experiments using Nedd4-2 WW domain peptide showed that the second WW domain of Nedd4-2 (2nd WW) is critical for binding to Kir5.1 (Fig.2B) comparing with the other three WW domains of Nedd4-2. Fig. 2B is a bar graph showing the normalized bands density ratio calculated from three separate pull-down experiments demonstrating that the second WW domain serves as the main binding site for Kir5.1. The calculated ratio was 1.00±0.07 (1st WW) , 11.64±0.93 (2nd WW), 0.73±0.02 (3rd WW) and 1.30±0.02 (4th WW), respectively (mean±SD $p<0.01$ for

2nd WW : 1st WW, 3nd WW or 4th WW). Thus, our experiments strongly suggest that Nedd4-2 is a binding partner for Kir5.1 or Kir4.1/Kir5.1 and that the second WW domain of Nedd4-2 is a major binding site for Kir5.1.

Ubiquitination of Kir4.1 by Nedd4-2 requires Kir5.1.   Having demonstrated the interaction between Nedd4-2 and Kir5.1, we further examined whether Nedd4-2 is able to ubiquitinate Kir5.1 or Kir4.1/5.1. Thus, we conducted ubiquitination assay using HEK293 transfected with Flag-Kir4.1/myc-Kir5.1/HA-Nedd4-2 or Flag-Kir5.1/myc-Kir4.1/HA-Nedd4-2. We used Flag antibody for immunoprecipitating Kir4.1 or Kir5.1 and Ub4D1 antibody for detecting ubiquitinated K channels. Fig.3A is a typical Western blot from five similar experiments showing that Nedd4-2 was not able to ubiquitinate Kir4.1 or Kir5.1 but it stimulated the ubiquitination of Kir4.1/Kir5.1 heterotetramer. Considering that Kir5.1 binds to Nedd4-2, we suspected that Nedd4-2 ubiquitinates Kir4.1 only in the presence of Kir5.1. This notion was also suggested by ubiquitination assay of Kir4.1 using denatured IP (same procedure described in Fig. 3A except for the pretreatment with 2% SDS before adding Flag antibody for IP). Fig. 3B is a representative western blot from three separate IP showing that Nedd4-2 enhanced Kir4.1 ubiquitination in the presence of Kir5.1. Slightly increased ubiquitination with Kir4.1/Kir5.1, Kir5.1/Nedd4-2 and 4.1/Nedd4-2 may be due to some endogenous proteins involving in ubiquitination. Since Kir4.1 is responsible for forming the K-conductive pathway of Kir4.1/5.1 (18), Nedd4-2-induced ubiquitination of Kir4.1/5.1 is expected to inhibit K channel activity. Thus, we next examined the effect of Nedd4-2 on Kir4.1 using the whole-cell recording in HEK293 cells transfected with GFP/HA-tagged Kir4.1 and Kir5.1 in the presence or absence of Nedd4-2. Twenty-four hours after transfection, GFP-positive cells were selected for the patch-clamp experiments. The cells were bathed with symmetrical 145 mM K solution (140 mM KCl and 5 M KOH) and the Ba^{2+} –sensitive K currents were measured with step protocol from -60 mV to 60 mV at 20 mV step. Fig.4A and 4B are two recordings showing Ba^{2+}-sensitive K currents in the cells transfected with Kir4.1+Kir5.1 and Nedd4-2+Kir4.1/5.1 respectively. Results from six experiments are summarized in Fig.4C showing that Nedd4-2 inhibits Kir4.1/5.1 channels and significantly decreased Ba^{2+}-sensitive K currents from 9300±290 pA to

5600±110 pA. The effect of Nedd4-2 on Kir4.1 was specific because co-expression of Kir5.1 and Nedd4-1 did not reduce Kir4.1 activity (9030±160 pA). In addition, dominant-negative Nedd4-2 (Nedd4-2DN, Nedd4-2C821A), an enzyme-inactivated form of Nedd4-2, failed to inhibit Kir4.1/5.1 (9250±290 pA) (Fig. 4C).

Having demonstrated that Nedd4-2 but not Nedd4-1decreases Kir4.1/5.1 K currents, we next used western blot to examine whether the inhibitory effect of Nedd4-2 on Kir4.1/5.1 was due to decreasing the expression of Kir4.1. Fig.5A is a western blot showing the expression of Kir4.1 in the cells transfected with Kir4.1+Nedd4-2, Kir4.1/5.1+Nedd4-2, Kir4.1+Nedd4-1 and Kir4.1/5.1+Nedd4-1. Fig. 5B is a bar graph showing the normalized band density of Kir4.1 expression which was reduced by the coexpression of Kir5.1 and Nedd4-2. While the expression of Kir4.1 in the cells transfected with Kir4.1 alone was similar to those with Kir4.1+Nedd4-2 (data not shown), Nedd4-2 decreased Kir4.1 expression by 55±10% (n=4) in comparison to the control (Kir4.1+Nedd4-2). In contrast, Nedd4-1 had no effect on the expression of Kir4.1. Thus, the results from western blots are consistent with electrophysiological results supporting the notion that the inhibitory effect of Nedd4-2 on Kir4.1 requires Kir5.1. Since TPVT motif on Kir5.1 is critical for interacting with Nedd4-2, we next studied the role of TPVT motif of Kir5.1 in Nedd4-2-mediated Kir4.1inhibition using patch-clamp technique in HEK293 cells transfected with Kir4.1/Nedd4-2/Kir5.1 or Kir5.1 mutants. Results of 6 experiments are summarized in Fig. 5C showing that the expression of Kir5.1^{T249A} largely abolished the inhibitory effect of Nedd4-2 on Kir4.1 (Kir4.1/5.1, 9330±250 pA; Kir4.1/5.1+Nedd4-2, 5500±170 pA; Kir4.1/5.1^{T249A} + Nedd4-2, 8600±270 pA). However, the expression of Kir5.1^{T249D} restored Nedd4-2-induced inhibition of Kir4.1 (5200±280 pA) while Ba^{2+}-sensitive K currents in cells transfected with Kir4.1/5.1^{T249A} (9100±200 pA) or Kir4.1/5.1^{T249D} (9000±270 pA) were similar to Kir4.1/5.1 (Fig.5D). This indicates that TPVT motif of Kir5.1 is important for Nedd4-2-induced Kir4.1 inhibition.

Deletion of Kir5.1 increases Kir4.1 currents and expression in DCT. After demonstrating that Kir5.1 plays a key role in mediating the inhibitory effect of Nedd4-2 on the Kir4.1 channel activity in

HEK293 cells, we next examined the role of Kir5.1 in the regulation of Kir4.1 in vivo. It is well established that Kir5.1 interacts with Kir4.1 to form a 40 pS inwardly rectifying K channel in the basolateral membrane of the DCT (18). Since the 40 pS K channel is the only type of K channel in the early part of the DCT (DCT1), the whole-cell K currents in DCT1 are equal to Kir4.1 which is responsible for forming K conductive pathway of Kir4.1/5.1 heterotetramer. Fig.6A is a trace of Ba^{2+}-sensitive K currents measured with RAMP protocol from -100 to 100 mV in DCT1 of WT and $Kir5.1^{-/-}$ mice (Kir5.1KO). It is apparent that whole-cell K currents in the DCT1 of $Kir5.1^{-/-}$ mice are larger than those of WT mice. The results from seven experiments are summarized in Fig. 6B showing that Ba^{2+}–sensitive K^+ currents measured at -60 mV were 1300±100 pA (WT) and 2200±280 pA ($Kir5.1^{-/-}$), respectively. Since the DCT K currents were measured at DCT1 where no ROMK activity was detected, therefore, the whole-cell K currents represent Kir4.1 activity(28; 34). Thus, the deletion of Kir5.1 significantly augments the basolateral Kir4.1 activity. This notion was also supported by immunoblotting to examine Kir4.1 expression in the kidney from $Kir5.1^{-/-}$ mice and the WT littermates. Fig. 6C is a western blot showing that the expression of Kir4.1 increased by 100±11% in $Kir5.1^{-/-}$ mice comparing with WT littermates (normalized with β-actin) (Fig. 6D). We also conducted immunofluorescent staining to examine the expression of Kir4.1 in the kidney from both WT and $Kir5.1^{-/-}$ mice. From inspection of Fig.6E, it is apparent that the fluorescence intensity of Kir4.1 staining is more intensified in $Kir5.1^{-/-}$ mice than WT littermates. Thus, electrophysiology, western blotting and immunostaining show that the deletion of Kir5.1 stimulates Kir4.1currents and expression in the DCT.

Deletion of Nedd4-2 increases Kir4.1currents and activity in DCT. If the deletion of Kir5.1-induced increase in Kir4.1 activity in the DCT depends on Nedd4-2 activity, we speculate that deletion of Nedd4-2 should mimic the effect of Kir5.1 deletion and increase Kir4.1 activity in the DCT. Thus, we used patch-clamp technique (Fig.7A), western blot (Fig.7B) and immunostaining (Fig.7C) to examine Kir4.1 in WT and kidney-specific Nedd4-2 knockout mice (Ks-Nedd4-2KO). Ks-Nedd4-2 KO mice were generated by doxycycline-treatment for two weeks and western blot shows that Nedd4-2 expression was completely eliminated in doxycycline-treated mice while it was present in untreated (control) mice. Fig. 7A summarizes

11

the result of 6 experiments in which the Ba^{2+}-sensitive K currents were measured in the DCT of WT and Ks-Nedd4-2 KO mice with the whole cell-recording. We observed that the whole-cell K currents measured at -60 mV was 1270±150 pA (WT mice) and 1980±250 pA (Ks-Nedd4-2 KO mice), respectively. Having shown that deletion of Nedd4-2 increased Kir4.1 currents in the DCT, we then examined the expression of Kir4.1 and Kir5.1 by western blot in WT and Ks-Nedd4-2 KO mice (Fig. 7B). It is apparent that the depletion of Nedd4-2 significantly increases the expression of Kir4.1 by 90±10% (n=4) but it did not significantly change the expression of Kir5.1 in comparing with WT control. In addition, we carried out immunostaining to examine Kir4.1 expression in Ks-Nedd4-2 KO mice and WT littermates (Fig.7C). It shows that the staining of Kir4.1 is increased in Ks-Nedd4-2 KO mice comparing with WT littermates. Thus, deletion of Nedd4-2 stimulates Kir4.1 expression and augments the basolateral K conductance of the DCT.

Discussion

The main finding of the present study is that Nedd4-2 ubiquitinates Kir4.1/5.1 heterotetramer and decreases Kir4.1 currents in the presence of Kir5.1. A similar study has been reported. Ekberg et all have reported that C-terminal region of the KCNQ3 subunit is required for the Nedd4-2-mediated ubiquitination of voltage-gated K(+) channels KCNQ2/3 and KCNQ3/5 (7). Two lines of evidence suggest that Kir5.1 is a binding partner of Nedd4-2: 1) CO-IP experiments showed that Nedd4-2 was immunoprecipitated with Kir5.1; 2) GST pull-down experiments demonstrated that Nedd4-2 was associated with Kir5.1. Since Kir5.1 is known to interact with Kir4.1 (18), it is possible that Kir5.1 plays a role in regulating the ubiquitination of Kir4.1/Kir5.1 by Nedd4-2. Nedd4-2 encoded by *Nedd4l* gene is a member of Nedd4 E3 ubiquitin ligase (21). Nedd4-2 has four WW domains which interact with PY motif or phosphor-serine or threonine-based motif of the substrate proteins and facilitates their ubiquitination and degradation (11; 15; 27). A large body of evidence has demonstrated that Nedd4-2 regulates the ubiquitination of ENaC through the interaction of PY motif in the β- and γENaC subunits with WW domains of Nedd4-2 (6; 11; 24; 26). Although Kir5.1 lacks a typical PY motif, it contains a TPVT motif at its c-terminus (AA 249 to 252). This motif is a

phosphothreonine-based binding motif of Nedd4 which has been shown to interact with M-phase inducer phosphatase 3 encoded by *Cdc25c* (15) and it is also highly preserved in Kir5.1 from humans, rats to mice. The observation that the expression of Kir5.1^{T249A} largely attenuated while the expression of Kir5.1^{T249D} enhanced the association between Kir5.1 and Nedd4-2 strongly suggests the critical role of TPVT sequence in the interaction between Nedd4-2 and Kir5.1. Moreover, the results from GST-pull-down further confirm that the second WW domain of Nedd4-2 is a major binding site for Kir5.1-Nedd4-2 association. Also, the observation that Nedd4-1 failed to mimic the effect of Nedd4-2 on Kir4.1 suggests that Nedd4-2 is the E3 ubiquitin ligase regulating Kir4.1/Kir5.1.

Although Nedd4-2 binds to Kir5.1, it is unlikely that Nedd4-2 facilitates the ubiquitination of Kir5.1 protein since coexpression of Nedd4-2 and Kir5.1 failed to change Kir5.1 ubiquitination. This notion is also supported by the finding that the deletion of Nedd4-2 had no effect on Kir5.1 expression in the kidney. Several lines of evidence suggest that the interaction of Nedd4-2 with Kir5.1 plays a key role in regulating Kir4.1 activity by ubiquitination. First, Nedd4-2 stimulates the ubiquitination of Kir4.1/Kir5.1 while it had no effect on Kir4.1 ubiquitination in the absence of Kir5.1. Second, Nedd4-2 decreases Kir4.1 expression and Kir4.1 currents only in the presence of Kir5.1. Third, deletion of either Kir5.1 or Nedd4-2 stimulates the basolateral K conductance and increases Kir4.1 expression in the native DCT. Our observation that the deletion of Kir5.1 increased the basolateral K conductance in the DCT is consistent with the report that *Kir5.1$^{-/-}$* mice displayed an increased basolateral K channel activity in the DCT(17). Although it is possible that reduced pH-sensitive may also contribute to the stimulation of Kir4.1 activity in *Kir5.1$^{-/-}$* mice, the observation that Kir5.1^{T249A} abolished the inhibition effect of Nedd4-2 on Kir4.1 implies that Kir5.1/Nedd4-2 interaction plays a role in regulating Kir4.1. This notion was also strongly supported by the observation that basolateral K conductance and Kir4.1 expression were increased in the DCT of Ks-Nedd4-2 KO mice. Fig. 8 is a scheme illustrating the mechanism by which Nedd4-2 interaction with Kir5.1 regulates Kir4.1. Nedd4-2 binds to TPVT motif of Kir5.1 thereby facilitating the ubiquitination of Kir4.1. The model of recognition in *trans* via an ancillary protein in ubiquitination system has been previously studied (7; 9). The

ubiquitinated Kir4.1 is expected to be endocytosed and degraded thereby decreasing the basolateral K channels in the DCT. The finding that deletion of Nedd4-2 did not alter the Kir5.1 expression suggests the possibility that Kir5.1 could be recycled and reused in forming Kir4.1/Kir5.1 heterotetramer. Thus, the inhibitory effect of Nedd4-2 on Kir4.1 mainly depends on the interaction between Nedd4-2 and Kir5.1.

Kir4.1 is expressed in the basolateral membrane of the late thick ascending limb (TAL), the DCT, connecting tubule (CNT) and cortical collecting duct (CCD)(4; 29; 33). Although Kir4.1 can form a low conductance (12-20 pS) homotetramer K channel in the absence of Kir5.1 (17; 18), it is well-documented that under physiological conditions, Kir4.1 interacts with Kir5.1 to form a 40 pS inwardly-rectifying K channel expressed in the basolateral membrane of TAL, DCT, CNT and CCD(3; 4; 12; 14). However, unlike in the TAL and in the CCD, this 40 pS K channel is the only type of K channel in the basolateral membrane of the DCT and plays a key role in generating negative membrane potential and K recycling(4; 34). Our previous experiments have demonstrated that Kir4.1 plays a dominant role in determining the basolateral K conductance in the DCT because disruption of Kir4.1 almost completely eliminates basolateral K conductance(4).

The physiological significance of our finding is to illustrate the role of Kir5.1 and Nedd4-2 interaction in regulating the basolateral Kir4.1 conductance of the DCT. DCT is responsible for reabsorption of 5% of the filtered sodium load and plays a key role in regulating renal K excretion in the aldosterone-sensitive distal nephron (ASDN) (8; 16). Recently, a large body of evidence suggests that thiazide-sensitive Na-Cl cotransporter (NCC) plays a key role in regulating renal K excretion (20; 23; 25; 31). For instance, hyperkalemia-induced decrease in NCC activity should increase sodium and volume delivery to the latter part of ASDN thereby stimulating K excretion. Conversely, hypokalemia-induced stimulation of NCC activity should decrease sodium and volume delivery to the ASDN thereby inhibiting K excretion in ASDN. Thus, the regulation of NCC is important for proper regulation of renal K excretion and K homeostasis. A high NCC activity has been shown to be related to Familial Hyperkalemic Hypertension while a low NCC activity has been demonstrated to be responsible for hypokalemia in Gitelman's syndrome (10; 23; 30). Our

previous study has demonstrated that Kir4.1 plays a key role in mediating the effect of dietary K intake on NCC activity (32). We have demonstrated that hyperkalemia-induced inhibition of the basolateral Kir4.1 is essential for the down-regulation of NCC while hypokalemia-induced stimulation of the basolateral Kir4.1 plays a critical role in stimulating NCC(32). It is most likely Cl-sensitive With-No-Lysine kinase (WNK) links the basolateral Kir4.1 activity to apical NCC activity (2; 19). Because Kir4.1 plays a role in regulating NCC, it is conceivable that Kir5.1 and Nedd4-2 interaction may play an important role in mediating the effect of dietary K intake on the basolateral K conductance in the DCT. This notion is supported by the report that NCC activity is upregulated in Kir5.1 KO mice and Ks-Nedd4-2 KO mice (17; 22). Our study also raises the possibility whether dietary K intake may also regulate the expression of Nedd4-2 thereby affecting NCC. However, further experiments are needed to explore this possibility. Thus, the modulation of Kir4.1 mediated by Nedd4-2/Kir5.1 interaction should expand our understanding the mechanism by which Kir4.1 regulates NCC function and K excretion. We conclude that Nedd4-2 ubiquitinates Kir4.1 through binding to Kir5.1 at TPVT motif and that the interaction between Kir5.1 and Nedd4-2 regulates basolateral Kir4.1 channel activity in DCT.

Disclosures

No conflicts of interest, financial or otherwise, are declared by the authors of this article.

Author contributions

DHL designed the study, performed experiments including protein-interaction and western blot, and wrote the paper. MXW, XTS and PW performed whole-cell recording patch-clamp, animal genotyping and breeding. ZXG performed immunostaining. OS and WHW read and edited the manuscript. All authors analyzed the results and approved the final version of the manuscript.

Reference List

1. **Amanchy R, Periaswamy B, Mathivanan S, Reddy R, Tattikota SG and Pandey A**. A curated compendium of phosphorylation motifs. *Nat Biotech* 25: 285-286, 2007.

2. **Bazua-Valenti S, Chavez-Canales M, Rojas-Vega L, Gonzalez-Rodriguez X, Vazquez N, Rodriguez-Gama A, Argaiz ER, Melo Z, Plata C, Ellison DH, Garcia-Valdes J, Hadchouel J and Gamba G**. The Effect of WNK4 on the Na+Cl Cotransporter Is Modulated by Intracellular Chloride. *J Am Soc Nephrol* 26: 1781-1786, 2014.

3. **Cha SK, Huang C, Ding Y, Qi X, Huang CL and Miller RT**. Calcium-sensing Receptor Decreases Cell Surface Expression of the Inwardly Rectifying K+ Channel Kir4.1. *J Biol Chem* 286: 1828-1835, 2011.

4. **Cuevas CA, Su XT, Wang MX, Terker AS, Lin DH, McCormick JA, Yang C-L, Ellison DH and Wang WH**. Potassium sensing by renal distal tubules requires Kir4.1. *J Am Soc Nephrol* 28: 1814-1825, 2017.

5. **Dawson DC and Richards NW**. Basolateral K conductance: Role in regulation of NaCl absorption and secretion. *Am J Physiol* 259: C181-C195, 1990.

6. **Debonneville C, Flores SY, Kamynina E, Plant PJ, Tauxe C, Thomas MA, Munster C, Chraibi A, Pratt JH, Horisberger JD, Pearce D, Loffing J and Staub O**. Phosphorylation of Nedd4-2 by Sgk1 regulates epithelial Na+ channel cell surface expression. *EMBO J* 20: 7052-7059, 2001.

7. **Ekberg J, Schuetz F, Boase NA, Conroy SJ, Manning J, Kumar S, Poronnik P and Adams DJ**. Regulation of the Voltage-gated K+ Channels KCNQ2/3 and KCNQ3/5 by Ubiquitination: NOVEL ROLE FOR Nedd4-2. *Journal of Biological Chemistry* 282: 12135-12142, 2007.

8. **Ellison DH, Valazquez H and Wright FS**. Thiazide-sensitive sodium chloride cotransport in early distal tubule. *Am J Physiol (Renal Fluid Electrolyte Physiol)* 253-22: F546-F554, 1987.

9. **Glickman MH and Ciechanover A**. The Ubiquitin-Proteasome Proteolytic Pathway: Destruction for the Sake of Construction. *Physiological Reviews* 82: 373-428, 2002.

10. **Grimm PR, Coleman R, Delpire E and Welling PA**. Constitutively active SPAK causes hyperkalemia by activating NCC and remodeling distal tubules. *J Am Soc Nephrol* 28: in press, 2017.

11. **Kamynina E and Staub O**. Concerted action of ENaC, Nedd4-2, and Sgk1 in transepithelial Na+ transport. *AJP - Renal Physiology* 283: F377-F387, 2002.

12. **Lachheb S, Cluzeaud F, Bens M, Genete M, Hibino H, Lourdel S, Kurachi Y, Vandewalle A, Teulon J and Paulais M**. Kir4.1/Kir5.1 channel forms the major K+ channel in the basolateral membrane of mouse renal collecting duct principal cells. *AJP - Renal Physiology* 294: F1398-F1407, 2008.

13. **Lin DH, Sterling H, Wang Z, Babilonia E, Yang B, Dong K, Hebert SC, Giebisch G and Wang WH**. ROMK1 channel activity is regulated by monoubiquitination. *Proc Natl Acad Sci* 0: 0, 2005.

14. **Lourdel S, Paulais M, Cluzeaud F, Bens M, Tanemoto M, Kurachi Y, Vandewalle A and Teulon J**. An inward rectifier K^+ channel at the basolateral membrane of the mouse distal convoluted tubule: similarities with Kir4-Kir5.1 heteromeric channels. *J Physiol* 538: 391-404, 2002.

15. **Lu PJ, Zhou XZ, Shen M and Lu KP**. Function of WW domains as phosphoserine- or phosphothreonine-binding modules. *Science* 283: 1325-1328, 1999.

16. **Obermuller N, Bernstein P, Velazquez H, Reilly R, Moser D, Ellison DH and Bachmann S**. Expression of the thiazide-sensitive Na-Cl cotransporter in rat and human kidney. *Am J Physiol* 269: F900-F910, 1995.

17. **Paulais M, Bloch-Faure M, Picard N, Jacques T, Ramakrishnan SK, Keck M, Sohet F, Eladari D, Houillier P, Lourdel Sp, Teulon J and Tucker SJ**. Renal phenotype in mice lacking the Kir5.1 (Kcnj16) K+ channel subunit contrasts with that observed in SeSAME/EAST syndrome. *Proceedings of the National Academy of Sciences* 108: 10361-10366, 2011.

18. **Pessia M, Tucker SJ, Lee K, Bond CT and Adelman JP**. Subunit positional effects revealed by novel heteromeric inwardly rectifying K^+ channels. *EMBO J* 15: 2980-2987, 1996.

19. **piala AT, Moon TM, Akella R, He HX, Cobb MH and Goldsmith EJ**. Chloride sensing by WNK1 involves inhibition of autophosphorylation. *Sciencesignaling* 7: ra41, 2014.

20. **Rengarajan S, Lee DH, Oh YT, Delpire E, Youn JH and McDonough AA**. Increasing plasma K+ by intravenous potassium infusion reduces NCC phosphorylation and drives kaliuresis and natriuresis. *American Journal of Physiology - Renal Physiology* 306: F1059-F1068, 2014.

21. **Rizzo F and Staub O**. NEDD4-2 and salt-sensitive hypertension. *Current Opinion in Nephrology and Hypertension* 24: 2015.

22. **Ronzaud C, Loffing-Cueni D, Hausel P, Debonneville A, Malsure SR, Fowler-Jaeger N, Boase NA, Perrier R, Maillard M, Yang B, Stokes JB, Koesters R, Kumar S, Hummler E, Loffing J and Staub O**. Renal tubular NEDD4-2 deficiency causes NCC-mediated salt-dependent hypertension. *J Clin Invest* 123: 657-665, 2013.

23. **Simon DB**. Gitelman's variant of Bartter's syndrome, inherited hypokalaemic alkalosis, is caused by mutations in the thiazide-sensitive Na[ndash]CI cotransporter. *Nature Genet* 12: 24-30, 1996.

24. **Snyder PM, Olson DR and Thomas BC**. Serum and Glucocorticoid-regulated Kinase Modulates Nedd4-2-mediated Inhibition of the Epithelial Na+Channel. *J Biol Chem* 277: 5-8, 2002.

25. **Sorensen MV, Grossmann S, Roesinger M, Gresko N, Todkar AP, Barmettler G, Ziegler U, Odermatt A, Loffing-Cueni D and Loffing J**. Rapid dephosphorylation of the renal sodium chloride cotransporter in response to oral potassium intake in mice. *Kidney Int* 83: 811-824, 2013.

26. **Staub O, Gautschi I, Ishikawa T, Breitschopf K, Ciechanover A, Schild L and Rotin D**. Regulation of stability and function of the epithelial Na$^+$ channel (ENaC) by ubiquitination. *The EMBO Journal* 16: 6325-6336, 1997.

27. **Staub O and Rotin D**. Role of Ubiquitylation in Cellular Membrane Transport. *Physiol Rev* 86: 669-707, 2006.

28. **Su XT and Wang WH**. The expression, regulation and function of Kir4.1 (Kcnj10) in the mammalian kidney. *American Journal of Physiology - Renal Physiology* 311: F12-F15, 2016.

29. **Su XT, Zhang C, Wang L, Gu R, Lin DH and Wang WH**. Disruption of KCNJ10 (Kir4.1) stimulates the expression of ENaC in the collecting duct. *American Journal of Physiology - Renal Physiology* 310: F985-F993, 2016.

30. **Take C, Ikeda K, Kurasawa T and Kurokawa K**. Increased Chloride Reabsorption as an Inherited Renal Tubular Defect in Familial Type II Pseudohypoaldosteronism. *N Engl J Med* 324: 472-476, 1991.

31. **Terker A-S, Zhang C, McCormick J-A, Lazelle R-A, Zhang C, Meermeier N-P, Siler D-A, Park H-J, Fu Y, Cohen D-M, Weinstein A-M, Wang WH, Yang CL and Ellison D-H**. Potassium Modulates Electrolyte Balance and Blood Pressure through Effects on Distal Cell Voltage and Chloride. *Cell Metabolism* 21: 39-50, 2015.

32. **Wang MX, Cuevas-Gallardo C, Su XT, Wu P, Gao Z-X, Lin DH, McCormick JA, Yang CL, Wang WH and Ellison DH**. Potassium (K+) intake modulates NCC activity via the K+ channel. Kir4.1. *Kid Int* 00: 00, 2017.

33. **Zhang C, Wang L, Su XT, Lin DH and Wang WH**. KCNJ10 (Kir4.1) is expressed in the basolateral membrane of the cortical thick ascending limb. *American Journal of Physiology - Renal Physiology* 308: F1288-F1296, 2015.

34. **Zhang C, Wang L, Thomas S, Wang K, Lin DH, Rinehart J and Wang WH**. Src-family protein tyrosine kinase regulates the basolateral K channel in the distal convoluted tubule (DCT) by phosphorylation of KCNJ10. *J Biol Chem* 288: 26135-26146, 2013.

35. **Zhang C, Wang L, Zhang J, Su X-T, Lin DH, Scholl UI, Giebisch G, Lifton RP and Wang WH**. KCNJ10 determines the expression of the apical Na-Cl cotransporter (NCC) in the early distal convoluted tubule (DCT1). *Proc Natl Acad Sci USA* 111: 11864-11869, 2014.

36. **Zhou R, Patel SV and Snyder PM**. Nedd4-2 Catalyzes Ubiquitination and Degradation of Cell Surface ENaC. *J Biol Chem* 282: 20207-20212, 2007.

Figure legends

Fig. 1 Nedd4-2 interacts with Kir5.1. (A) Co-immunoprecipitation experiments (Co-IP) show the interaction of Kir5.1 with Nedd4-2 or Nedd4-1 in HEK293 cells transfected with HA-GFP-Kir5.1 and Flag-tagged Nedd4-2 or Nedd4-1 (top panel). Middle panel shows the equal amount of Flag-Nedd4-2 and –Nedd4-1 used for Co-IP. Lower panel shows the input of HA-GFP-Kir5.1. (B) Co-IP shows the interaction of Nedd4-2 or Nedd4-1 with Kir5.1 in HEK293 cells transfected with myc-Kir5.1 and Flag-tagged-Nedd4-2. Lower panel shows the equal amount of myc-Kir5.1 used for Co-IP. An unspecific band is indicated by a star. Cells transfected with myc-Kir5.1 are used as negative control (Labelled as Kir5.1). (C) Co-IP shows that interaction of Nedd4-2 and Kir5.1/mutants in HEK293 cells transfected with Flag-tagged-Nedd4-2 and HA-GFP-Kir5.1 or mutants (Kir5.1^{T249A} or Kir5.1^{T249D}) (Top panel). Middle panel shows the equal amount of Flag-Nedd4-2 and –Nedd4-1 used for Co-IP. Lower panel shows the input of HA-GFP-Kir5.1. Cells transfected with empty vector are used as IgG control (labelled as IgG). Cells transfected with Flag-Nedd4-2 are used as negative control (Labelled as Nedd4-2). (D) Co-IP shows that interaction of Nedd4-2 and Kir5.1/mutants in HEK293 cells transfected with Flag-tagged-Nedd4-2 and HA-GFP-Kir5.1 or mutants (Kir5.1^{T252A} or Kir5.1^{T252D}) (Top panel). Middle panel shows the amount of Flag-Nedd4-2 used for Co-IP. Lower panel shows the input of HA-GFP-Kir5.1. (E) A bar graph illustrates the normalized band density for the results of CO-IP.

Fig. 2 The second WW domain of Nedd4-2 interacts with Kir5.1. (A) Glutathione agarose gel shows that flag-tagged Nedd4-2 is pulled down by GST-Kir5.1 (Top panel). GST-Kir5.1 and GST are indicated in middle panel and lower panel shows the input of Flag-tagged-Nedd4-2. Flag-Nedd4-2 (200µg) obtained from TNT T7 Quick Coupled Translation System was added for the experiments. GST protein was mixed with 50 µl of washed Glutathione beads. (B) GST-pull-down experiments using Nedd4-2-WW domain peptide show that His-Kir5.1-C-terminus containing TPVT motif (AA 249 to 252) prefers to interact with Nedd4-2 2nd WW domain peptide. Each of four WW domains of Nedd4-2 (Table 2) was cloned into pGEX4T-1 vector by PCR. A bar graph summarizing the above results is shown in the bottom panel.

Fig. 3 Kir 5.1 is required for Nedd4-2-mediated ubiquitination of Kir4.1. (A) Ubiquitination assay shows ubiquitinated K channel in HEK293 cells transfected with flag-tagged Kir4.1 or Kir5.1, Kir4.1+Nedd4-2, Kir4.1+Kir5.1, Kir5.1+Nedd4-2 and Kir4.1/5.1+ Nedd4-2, respectively. Flag antibody was used to immunoprecipitate Flag-tagged Kir4.1 or 5.1 and ubiquitin (Ub) antibody was used to detect ubiquitinated K channels (indicated by a bracket). (B) Ubiquitination assay with SDS pretreatment shows ubiquitinated K channels in HEK293 cells transfected with Flag-tagged Kir4.1, Kir4.1+Nedd4-2 and Kir4.1/5.1+Nedd4-2. Lower panel shows the expression of Kir4.1 used for IP.

Fig.4 Nedd4-2 but not Nedd4-1 inhibits Kir4.1/Kir5.1 channels. Whole-cell recording shows Ba^{2+}-sensitive K currents measured from -60 mV to 60 mV at -20 mV step in HEK293 cells transfected with Kir4.1+Kir5.1 (A) or with Kir4.1/5.1 +Nedd4-2 (B). The symmetrical 145 mM K solution was used for both bath and pipette. (C) A bar graph summarizes the results of experiments (n=6) in which Ba^{2+}-sensitive K currents were measured with whole-cell recording in HEK293 cells transfected with Kir4.1, Kir4.1+Nedd4-2, Kir4.1/5.1, Kir4.1/5.1+Nedd4-2, Kir4.1/5.1+Nedd4-1 and Kir4.1/5.1+dead Nedd4-2. The patch-clamp experiments were performed 24 hr after the transfection and the positive transfected cells were identified by GFP fluorescence.

Fig.5 Mutation of TPVT motif of Kir5.1 abolishes Nedd4-2-mediated inhibition of Kir4.1/5.1. (A) A western blot shows the expression of Kir4.1 in HEK293 cells transfected with Ki4.1+Nedd4-2, Kir4.1/5.1+Nedd4-2, Kir4.1+Nedd4-1 and Kir4.1/5.1+Nedd4-1. The expression of Nedd4 was shown in the middle panel. (B) The normalized band density of Kir4.1 expression is shown in a bar graph. (C) A bar graph summarizes the results of experiments in which Ba^{2+}-sensitive K currents were measured (at -60 mV) with whole-cell recording in HEK293 cells transfected with Kir4.1/5.1, Kir4.1/5.1+Nedd4-2, Kir4.1/5.1^{T249A}+Nedd4-2 and Kir4.1/5.1^{T249D} +Nedd4-2, respectively (n=6). (D) Ba^{2+}-sensitive K currents measured at -60 mV with whole-cell recording in HEK293 cells transfected with Kir4.1/5.1, Kir4.1/5.1^{T249A} and Kir4.1/5.1^{T249D} (n=6). The patch-clamp experiments were performed 24 hr after the transfection and symmetrical 145 mM K was used for the pipette and the bath solution.

Fig. 6 Deletion of Kir5.1 stimulates the basolateral Kir4.1 in the DCT. (A) A whole-cell recording showing Ba^{2+}-sensitive K currents in the DCT of the WT or Kir5.1 KO mice. The K currents were measured with a ramp protocol from -100 to 100 mV using symmetrical 145 mM K solution in the bath and pipette. **(B)** A bar graph summarizes the results of experiments in which Ba^{2+}-sensitive K currents of the DCT were measured at -60 mV from the WT and Kir5.1 KO mice (*n*=6). Western blot shows the expression of Kir4.1 in WT and Kir5.1 KO mice (C) and a bar graph summarizes normalized band density of Kir4.1 (D). (E) Immunostaining of Kir4.1 in kidney from WT and Kir5.1 KO mice. The treatment for the kidney slides was identical.

Fig. 7 Deletion of Nedd4-2 increases Kir4.1 expression. (A) A bar graph summarizes the results of experiments in which Ba^{2+}-sensitive K currents of the DCT were measured at -60 mV from the WT and Ks-Nedd4-2 KO mice (*n*=6). (B) Western blots showed the expression of Kir4.1 and Kir5.1 in WT and Ks-Nedd4-2 KO mice. A bar graph summarizes normalized band density of Kir4.1 and Ki5.1 (right panel). (C) Immunostaining of Kir4.1 in kidney from Ks-Nedd4-2 KO mice and WT control (without doxycycline treated).

Fig. 8 A scheme illustrating the role of Kir5.1 as a binding partner in mediating Nedd4-2 E3 ligase dependent degradation of Kir4.1 in the DCT. A part of Kir5.1 sequence (from AA241 to 260) including TPVT motif is shown on the top.

Table 1 Primers used for genotyping.

Kir4.1 Flox	Forward	TGATGTATCTCGATTGCTGC
	Reverse	CCCTACTCAATGCTCTTAAC
Nedd4-2 Flox	Nedd4-2 Forward	TGAGCTCATTGCTTCACTTCC
	Nedd4-2 Reverse	TTCATGCTCGAAGCCTTAGC
	Flox Reverse	TTTGTGAGGACAGCCTCTAGC
Pax8	Forward	CCATGTCTAGACTGGACAAGA
	Reverse	CTCCAGGCCACATATGATTAG
Cre	Forward	TCGCTGCATTACCGGTCGATGC
	Reverse	CCATGAGTGAACGAACCTGGTCG

Table 2 Primers used for cloning WW domains of nedd4-2 (Uniprot_Q96PU5) and C-terminal peptide of Kir5.1 (Q9NPI9_ AA168-418).

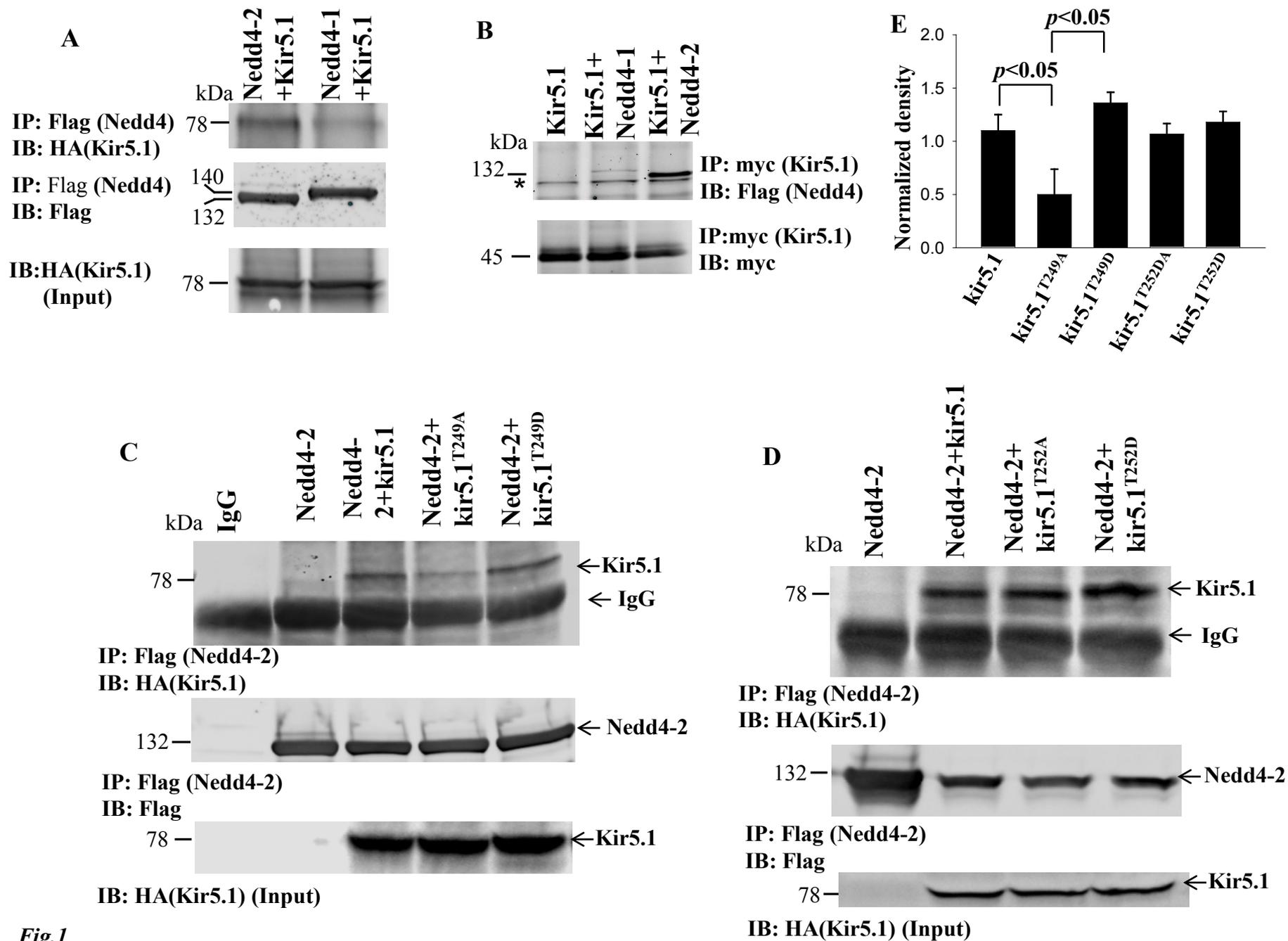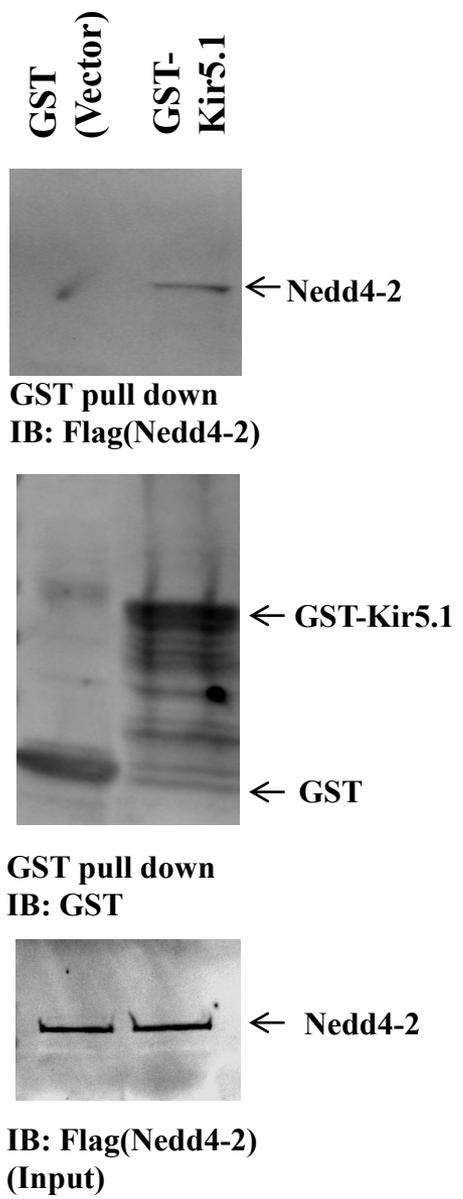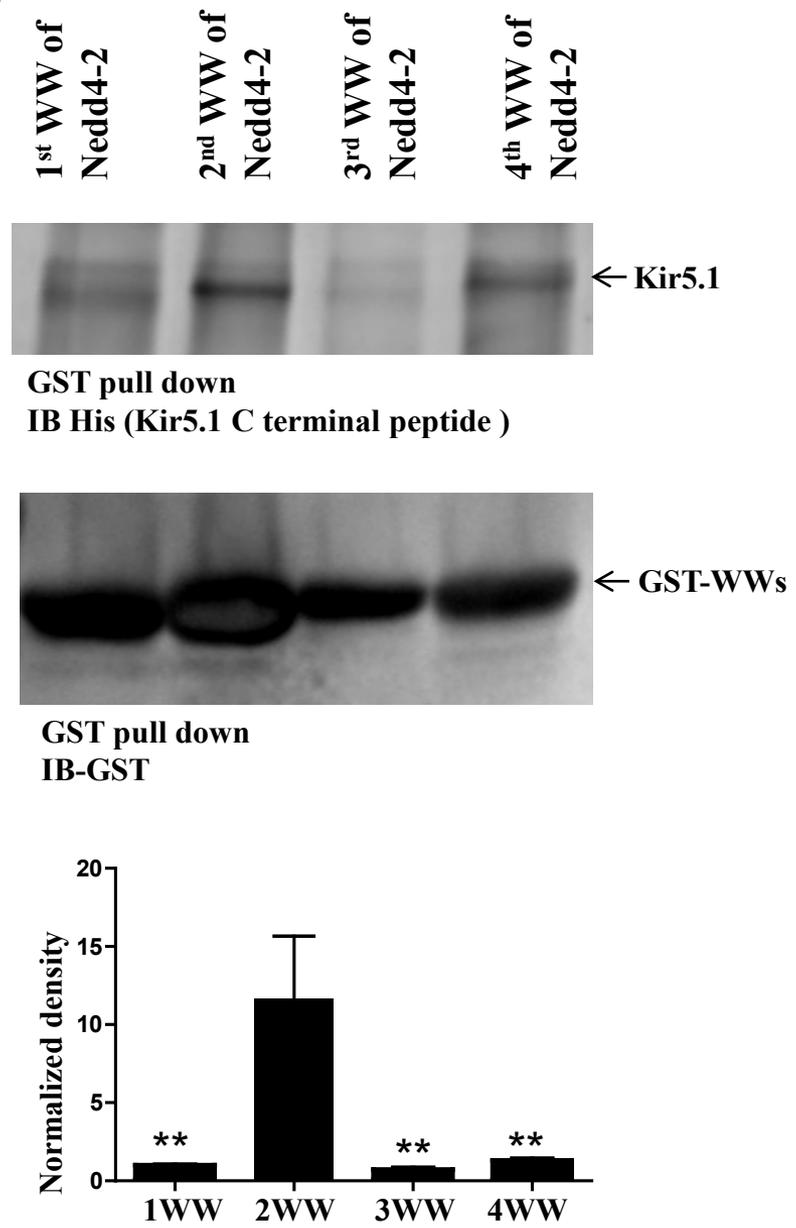|		
1WW	Forward	5'-ACGCGGATCCACCATGGGGTGGGAAGAAAAAGTGGAC
(81bp)	Reverse	5'-AGGGCTCGAGTTATGGTCTGTGCCACTGAGTG
2WW	Forward	5'-ACGCGGATCCACCATGCTGCCTTCAGGCTGGGAAG
(90bp)	Reverse	5'-AGGGCTCGAGTTAAGGTCGAGTCCAAGTTGTG
3WW	Forward	5'-ACGCGGATCCACCATGCCACCCGGCTGGGAAATG
(93bp)	Reverse	5'-AGGGCTCGAGTTACAAACGTGGATCTTCCCAG
4WW	Forward	5'-ACGCGGATCCACCATGCCCCTTCCTCCTGGCTGG
(99bp)	Reverse	5'-AGGGCTCGAGTTACAGTCTTGGGTCTTCCCAC
Kir5.1-C-ter	Forward	5'-AAAACATATGACCATG GCCTTGGCCAAAATGGCAACTGCTC
(756bp)	Reverse	5'- AAAGGATCCCATTTGGGATTCTACAGAG

A

IP: Flag (Nedd4)
IB: HA(Kir5.1)

IP: Flag (Nedd4)
IB: Flag

IB:HA(Kir5.1)
(Input)

B

IP: myc (Kir5.1)
IB: Flag (Nedd4)

IP:myc (Kir5.1)
IB: myc

C

IP: Flag (Nedd4-2)
IB: HA(Kir5.1)

IP: Flag (Nedd4-2)
IB: Flag

IB: HA(Kir5.1) (Input)

D

IP: Flag (Nedd4-2)
IB: HA(Kir5.1)

IP: Flag (Nedd4-2)
IB: Flag

IB: HA(Kir5.1) (Input)

E

Fig.1

A

GST
(Vector)

GST-
Kir5.1

← Nedd4-2

GST pull down
IB: Flag(Nedd4-2)

← GST-Kir5.1

← GST

GST pull down
IB: GST

← Nedd4-2

IB: Flag(Nedd4-2)
(Input)

B

1st WW of
Nedd4-2

2nd WW of
Nedd4-2

3rd WW of
Nedd4-2

4th WW of
Nedd4-2

← Kir5.1

GST pull down
IB His (Kir5.1 C terminal peptide)

← GST-WWs

GST pull down
IB-GST

Fig.2

A

IgG
Kir4.1
Kir4.1+Nedd4-2
Kir4.1+Kir5.1

IgG
Kir5.1
Kir5.1+Nedd4-2
Kir4.1+Kir5.1+Nedd4-2

Ub-Kir

IgG →

IP: Flag (Kir4.1)
IB: Ub

IP: Flag (Kir5.1)
IB: Ub

B

IgG
Kir4.1
Kir4.1+Nedd4-2
Kir4.1+Kir5.1+Nedd4-2

Ub-Kir

IP-Flag(Kir4.1)
IB-Ub

IP-Flag(Kir4.1)
IB-Flag

Fig.3

A

Kir4.1+Kir5.1

B

Nedd4-2 +Kir4.1+Kir5.1

5nA

100ms

60mV

-60mV

C

$p<0.05$

$p<0.05$

$p<0.05$

$p<0.05$

Ba^{2+}-sensitive K$^+$ currents (pA/30 pF)

10000

7500

5000

2500

0

Kir4.1

Kir4.1+Nedd4-2

Kir4.1+Kir5.1

Kir4.1/5.1+Nedd4-2

Kir4.1/5.1+Nedd4-1

Kir4.1/5.1+Nedd4-2(DN)

Fig.4

A

Kir4.1+Nedd4-2   Kir4.1/5.1+Nedd4-2   Kir4.1+Nedd4-1   Kir4.1/5.1+Nedd4-1

IB:HA(Kir4.1)

← Nedd4-1
← Nedd4-2

IB-Flag (Nedd4-2 or Nedd4-1)

IB-Tubulin

B

Normalized intensity of Kir4.1 (%)

$p<0.05$ $p<0.05$

Kir4.1+Nedd4-2   Kir4.1/5.1+Nedd4-2   Kir4.1+Nedd4-1   Kir4.1/5.1+Nedd4-1

C

Ba^{2+}-sensitive K$^+$ currents (pA/30 pF)

$p<0.05$ $p<0.05$ $p<0.05$

Kir4.1+Kir5.1   Kir4.1/5.1+Nedd4-2   Kir4.1/5.1^{T249A}+Nedd4-2   Kir4.1/5.1^{T249D}+Nedd4-2

D

Ba^{2+}-sensitive K$^+$ currents (pA/30 pF)

NS   NS

Kir4.1/Kir5.1   Kir4.1/Kir5.1^{T249A} Kir4.1/Kir5.1^{T249D}

Fig.5

A

WT

Kir5.1 KO

B

p<0.01

C

kDa

48 —

IB: Kir4.1

IB: β-actin

D

p<0.01

E

WT anti-4.1

Kir5.1 KO anti-4.1

50 μm

50 μm

Fig.6

Fig. 7

^{241}VNDQIILVTPVTIVHEIDHE^{260} (Kir5.1)(*Kcnj16*)

Ubiquitination

Endocytosis

Degradation

Recycling

TPVT motif

Nedd4-2

Fig. 8